

Suppression of mitochondrial NADP⁺-dependent isocitrate dehydrogenase activity enhances curcumin-induced apoptosis in HCT116 cells

KYU HO JUNG & JEEN-WOO PARK

School of Life Sciences and Biotechnology, College of Natural Sciences, Kyungpook National University, Taegu 702-701, Korea

(Received date: 9 July 2010; Accepted date: 12 November 2010)

Abstract

Curcumin is a polyphenol derived from the plant *Curcuma longa* that induces apoptotic cell death in malignant cancer cell lines. It has been shown previously that mitochondrial NADP⁺-dependent isocitrate dehydrogenase (IDPm) plays an essential role in defense against oxidative stress by supplying NADPH for antioxidant systems. This study demonstrates that curcumin decreased the activity of IDPm, both as a purified enzyme and in cultured cells. It also shows that curcumin-induced apoptosis in the colon cancer cell line HCT116 is significantly enhanced by suppression of IDPm activity. Transfection of HCT116 cells with an IDPm small interfering RNA (siRNA) markedly decreased activity of IDPm, enhancing cellular susceptibility to curcumin-induced apoptosis, as reflected by DNA fragmentation, cellular redox status, mitochondria dysfunction and modulation of apoptotic marker proteins. Together, these results suggest that application of curcumin together with IDPm siRNA may be an effective combination modality in the treatment of cancer.

Keywords: Antioxidant enzyme, siRNA, apoptosis, curcumin, redox status

Introduction

Curcumin is a natural lipid-soluble yellow pigment extracted from turmeric (*Curcuma longa*), a rhizome used in India for centuries as a spice and medicinal agent [1]. It possesses a wide range of biological and pharmacological properties. These include the ability to promote cell shrinkage, chromatin condensation and oxidative DNA damage [2]. Curcumin can also inhibit inflammatory processes [3] and act as an antioxidant [4]. It can inhibit tumour proliferation in cell lines [5] and animals [6] and, importantly, it has been shown to induce apoptosis in a range of malignant cancer cell lines [7]. The potential of curcumin as a cancer therapeutic has been widely studied and a number of mechanistic explanations for its activity have been proposed [1,8]. Recently, modification of thioredoxin reductase has been proposed as a potential mechanism for the anti-cancer effects of curcumin [9]. In this report, alkylation of cysteine and selenocysteine

residues of enzyme has been proposed as an inhibitory mechanism of curcumin.

Reactive oxygen species (ROS) are thought to regulate the processes involved in the initiation of apoptotic signalling [10]. To overcome lethal oxidative environments, cells have evolved a series of antioxidant defense systems. Despite these protective mechanisms, excessive production of ROS can lead to tissue injury and is associated with various diseases, including cancer [11]. In addition, if antioxidant enzymes are inactivated or down-regulated, the harmful effects of oxidative stress may be exacerbated. In this respect, a unique anti-tumour strategy can be envisaged that selectively induces excess oxidative stress in tumour cells or preferentially disrupts the antioxidative defense systems of tumour cells [11]. The primary defenses against ROS generated from mitochondria are mitochondrial manganese superoxide dismutase (MnSOD) [12],

Correspondence: J.-W. Park, School of Life Sciences and Biotechnology, College of Natural Sciences, Kyungpook National University, Taegu 702-701, South Korea. Fax: 82 53 943 2762. Email: parkjw@knu.ac.kr

glutathione peroxidase [13] and peroxiredoxin 3 [14]. Reduced glutathione (GSH) participates in cellular defense as a potent antioxidant, but also as a substrate for mitochondrial glutathione peroxidase and glutathione-dependent phospholipids hydroperoxidase [15]. GSH levels in mitochondria are maintained by NADPH-dependent glutathione reductase [16]. NADPH is also required for the regeneration of the thioredoxin system, which is essential for the maintenance of cellular thiol homeostasis [17]. In this context, mitochondrial NADPH is of fundamental importance in the defense against ROS. The isocitrate dehydrogenases (ICDHs, EC1.1.1.41 and EC1.1.1.42) catalyse the production of NADH or NADPH, from NAD⁺ or NADP⁺, through the oxidative decarboxylation of isocitrate, to α -ketoglutarate and require either NAD⁺ or NADP⁺, producing NADH and NADPH, respectively [18]. We have shown that mitochondrial ICDH (IDPm) is involved in the supply of NADPH needed for GSH production in response to mitochondrial oxidative damage [19]. Therefore, attenuation of IDPm activity may result in the perturbation of the redox homeostasis and it may increase the sensitivity of tumour cells to anti-cancer agents.

In the present report, we show that curcumin can inactivate IDPm by a mechanism likely to involve modification of sulphhydryl groups in the enzyme. We also report that specific inhibition of IDPm expression by a small interfering RNA (siRNA) led to enhanced curcumin-induced apoptosis in a colon cancer cell line. The application of IDPm siRNA as a sensitizer for curcumin-induced apoptotic cell death offers a promising therapeutic approach for the treatment of cancer.

Materials and methods

Materials

β -NADP⁺, isocitrate, curcumin, dithiothreitol (DTT), 5,5'-dithiobis(2-nitrobenzoic acid) (DTNB), GSH, N-acetylcysteine (NAC), propidium iodide (PI) and anti-rabbit IgG tetramethylrhodamine isothiocyanate (TRITC) conjugated secondary antibody were obtained from Sigma Chemical Co. (St. Louis, MO). *N,N'*-Dimethyl-*N*(iodoacetyl)-*N'*-(7-nitrobenz-2-oxa-1, 3-diazol-4-yl)ethyleneamine (IANBD), 2', 7'-dichlorofluorescein diacetate (DCFH-DA), dihydrorhodamine 123 (DHR 123) and rhodamine 123 were purchased from Molecular Probes (Eugene, OR). Antibodies were purchased from Santa Cruz (Santa Cruz, CA) and Cell Signaling (Beverly, MA). A peptide representing the N-terminal 16 amino acids of mouse IDPm (ADKRIKVAKPV-VEMPG) was used to prepare polyclonal anti-IDPm antibodies [19].

Vector construction

For the construction of the His-tagged IDPm purification vector pET14b-IDPm, a 1.3-kb DNA encoding the IDPm gene (*IDH2*) was amplified from LNCX containing the cDNA insert for IDPm by polymerase chain reaction. In brief, the 5'-primer oligonucleotide (5'-GGAATTCCATATGGCTGAGAAGAGGA-3'), which annealed to the 5' end of *IDH2* and introduced an NdeI site, and 3'-primer oligonucleotide (5'-CAGGATCCCTACTGCTTGCCCA-3'), complementary to the 3' terminus of *IDH2* but inserted as a BamHI site, were used as primers.

Site-directed mutagenesis and preparation of recombinant proteins

Site-directed mutagenesis was performed using the QuikChange site-directed mutagenesis kit (Stratagene, La Jolla, CA). The following mutagenic primers were used: 5'-GCTTTGTGTGGGCTTCCAAGA ACTATGATG-3' for C269S and 5'-GACCTGGCT GGTCTATCCATGGCCTCAG-3' for C379S, respectively, in which the substituted serine codon is underlined. To prepare recombinant proteins, *E. coli* transformed with pET14b containing the cDNA insert for mouse IDPm or mutant IDPm (C269S, C379S and C269S/C379S double mutant) constructs were grown and lysed and His-tagged proteins were purified on Ni-nitrilotriacetic acid agarose as described previously [20].

Cell culture and cytotoxicity

Cells were grown in Dulbecco's modified Eagle's medium supplemented with 10% FBS, 2 mM glutamine and 100 units/ml penicillin/streptomycin in an incubator containing a humidified atmosphere of 95% air and 5% CO₂ at 37°C. Cell viability following treatment with different concentrations of curcumin was determined by trypan blue dye exclusion test.

Knockdown of IDPm by siRNA

IDPm siRNA and control (scrambled) siRNA were purchased from Samchully Pharm (Seoul, Korea). The sequences of the dsRNAs of IDPm and control used in the current experiments are as follows. For IDPm, sense and antisense siRNAs are 5'-AGAC CGACUUCGACAAGAAAdTdT-3' and 5'-UUCUU GUCGAAGUCGGUCUdTdT-3', respectively. For scrambled control, sense and antisense siRNAs are 5'-CUGAUGACCUGAGUGAAUGdTdT-3' and 5'-CAUUCACUCAGGUCAUCAGdTdT-3', respectively. HCT116 cells were transfected with 20 nM oligonucleotide using Lipofectamine (Invitrogen) in serum-free conditions according to the manufacturer's

protocol. After incubation for 24 h, the cells were washed and supplemented with fresh medium containing 10% FBS.

Enzyme activity assays

IDPm (6.5 μg) was added to 1 ml Tris buffer, pH 7.4, containing NADP^+ (2 mM), MgCl_2 (2 mM) and isocitrate (5 mM). Activity of IDPm was measured by the production of NADPH at 340 nm at 25°C. For the determination of IDPm activity in HCT116 cells, the isolated mitochondrial pellets were resuspended in $1\times$ PBS containing 0.1% Triton-X100, disrupted by ultrasonication (4710 Series, Cole-Palmer, Chicago, IL) twice at 40% of maximum setting for 10 s and centrifuged at $15,000\times g$ for 30 min. The supernatant was used to measure the activity of IDPm. The enzymatic assay of caspase-3 was measured by using the manufacturer's protocol (Promega, Madison, WI). Briefly, cells were suspended in a lysis buffer (50 mM HEPES, pH 7.4, 100 mM NaCl, 0.1% CHAPS, 1 mM DTT and 0.1 mM EDTA) for 10 min at 0°C and centrifuged at $10,000\times g$ for 10 min at 4°C. The supernatant containing 100 μg protein was incubated with reaction buffer (100 mM HEPES, pH 7.4, 0.5 mM PMSF, 10 mM dithiothreitol, 1 mM EDTA and 10% glycerol) containing caspase colourimetric substrate DEVD-pNA and incubated for 2 h at 37°C. The absorbance was then monitored at 405 nm to determine the caspase activity.

IANBD labelling of IDPm

Purified IDPm was labelled with a 15-fold molar excess of IANBD in a total volume of 100 μl of buffer (50 mM Tris-HCl, pH 7.4/100 mM NaCl). The reaction was allowed to proceed for 1 h at room temperature in the dark. The labelled IDPm was analysed by 10% SDS-PAGE. Incorporated IANBD was visualized by photographing the gel under UV light.

Immunoblot analysis

Proteins were separated on 10–12.5% SDS-polyacrylamide gel, transferred to nitrocellulose membranes and subsequently subjected to immunoblot analysis using appropriate antibodies. Proteins were visualized by using horseradish peroxidase-labelled anti-rabbit IgG and an enhanced chemiluminescence detection kit (Amersham Pharmacia Biotech, Buckinghamshire, UK).

Cellular redox status

Intracellular peroxide production was measured by confocal microscopy of DCFH oxidation using DCFH-DA as a probe. Cells were grown at 2×10^6

cells per 100-mm plate containing slide glass coated with poly-L-lysine and maintained in the growth medium for 24 h. Cells were treated with 10 μM DCFH-DA for 15 min and cells on the slide glass were washed with PBS and a cover glass was put on the slide glass. 2',7'-Dichlorofluorescein (DCF) fluorescence (excitation, 488 nm; emission, 520 nm) was imaged by confocal microscopy. NADPH was measured using the enzymatic cycling method as described by Zerez et al. [21] and expressed as the ratio of NADPH to the total NADP pool. The concentration of total glutathione was determined by the rate of formation of 5-thio-2-nitrobenzoic acid at 412 nm ($\epsilon = 1.36\times 10^4\text{ M}^{-1}\text{cm}^{-1}$), and oxidized glutathione (GSSG) was measured by the DTNB-GSSG reductase recycling assay after treating GSH with 2-vinylpyridine [22].

DNA fragmentation

Cells were collected by centrifugation, resuspended in 250 μl 10 mM Tris and 1 mM EDTA, pH 8.0 (TE buffer) and incubated with one additional volume of lysis buffer (5 mM Tris, 20 mM EDTA and 0.5% Triton X-100, pH 8.0) for 30 min at 4°C. After lysis, the intact chromatin (pellet) was separated from DNA fragments (supernatant) by centrifugation for 15 min at $13,000\times g$. Pellets were resuspended in 500 μl TE buffer and samples were precipitated by adding 500 μl 10% trichloroacetic acid at 4°C. Samples were pelleted at $4000\times g$ for 10 min and the supernatant was removed. After addition of 300 μl 5% trichloroacetic acid, samples were boiled for 15 min. DNA content was quantitated using the diphenylamine reagent. The percentage of fragmented DNA was calculated as the ratio of the DNA content in the supernatant to the amount in the pellet.

FACS

For analysis of cell cycle distribution, HCT116 cells were collected at $2000\times g$ for 5 min and washed once with cold PBS, fixed in 70% ethanol, decant ethanol by centrifuge and stained with PI. Labelled nuclei were subjected to flow cytometric analysis and then gated on a light scatter to remove debris and the percentage of nuclei with a sub- G_1 content was considered apoptotic cells.

Mitochondrial redox status and damage

To determine the levels of mitochondrial ROS cells in PBS were incubated for 20 min at 37°C with 5 μM DHR 123 and cells loaded with the fluorescent probes were imaged with a fluorescence microscope. Mitochondrial membrane permeability transition (MPT) was measured by the incorporation of rhodamine 123

dye into the mitochondria, as previously described [23]. Cells were exposed to curcumin and then treated with 5 μ M rhodamine 123 for 15 min and excited at 488 nm with an argon laser.

Statistical analysis

The difference between two mean values was analysed by Student's *t*-test and was considered to be statistically significant when $p < 0.05$.

Results and discussion

IDPm is an essential enzyme in cellular defence against oxidative damage by supplying NADPH in the mitochondria [19]. We have shown previously that increased IDPm expression resulting from transfection of IDPm cDNA protected cells from apoptosis induced by various cellular conditions causing oxidative stress, including hyperglycaemia, heat shock and γ -irradiation [24–26]. Conversely, inhibition of IDPm activity by the specific competitive inhibitor oxalomalate or down-regulation of IDPm expression by antisense cDNA or IDPm siRNA enhanced apoptosis of cancer cells exposed to γ -irradiation, tumour necrosis factor- α and

staurosporine [26–28]. Therefore, we hypothesized that suppression of IDPm expression may sensitize cancer cells to curcumin-induced apoptosis.

When IDPm was incubated with curcumin, a concentration- and time-dependent loss of enzyme activity was observed (Figure 1A). The inclusion of 10 mM DTT or 10 mM GSH during incubation blocked the inhibition of IDPm by 50 μ M curcumin (Figure 1B), suggesting that curcumin targets cysteine residues of IDPm. To further confirm the reaction between cysteinyl thiol groups of IDPm and curcumin, IDPm was labelled with a sulphhydryl-specific fluorophore IANBD in the presence of curcumin. As shown in Figure 1C, the intensity of IANBD-labelled IDPm was decreased by curcumin in a concentration-dependent manner. It has been proposed that cysteine residues in IDPm could be potential targets of sulphhydryl modifying agents [29,30]. The total number of cysteine residues in mammalian IDPm has been reported to be 8.2–8.8 mol/mol sub-unit [31]. In these cysteines, Cys²⁶⁹ and Cys³⁷⁹ were regulated by N-ethylmaleimide and the main site of modified cysteines [29]. Cys²⁶⁹ has a catalytic role, most likely by promoting the binding of Mn²⁺ in the presence of isocitrate. Cys³⁷⁹ is not essential for catalysis, but is the binding site for NADP⁺ [29]. To identify which

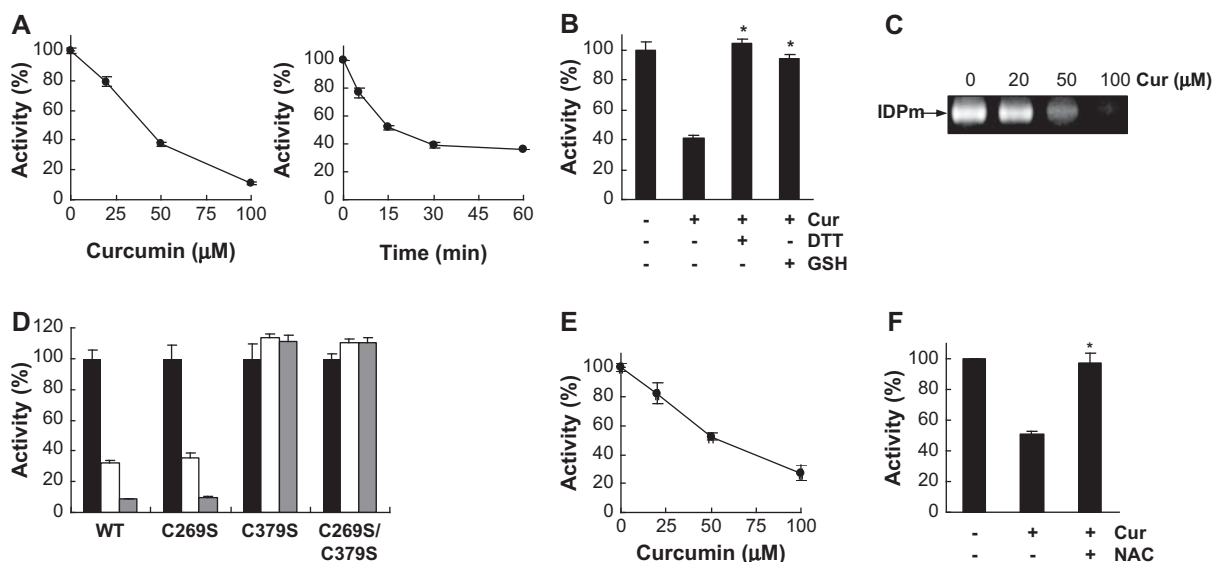


Figure 1. Inactivation of IDPm by curcumin. (A) IDPm was incubated with various concentrations of curcumin for 1 h or incubated with 50 μ M curcumin for various lengths of time and then IDPm activity was determined. Activities are given as a percentage of the control value. Data are presented as means \pm SD of three separate experiments. (B) Effect of thiols on the inactivation of IDPm by curcumin. After incubation of IDPm with 50 μ M curcumin in the presence of 10 mM DTT or 10 mM GSH for 1 h, activities of IDPm were determined. Data are presented as means \pm SD of three separate experiments; * $p < 0.01$ vs the enzyme exposed to curcumin. (C) IDPm was incubated with IANBD in the presence of curcumin for 1 h and the reaction mixture was subjected to 10% SDS-PAGE. Labelled IDPm was identified by photographing the gel under UV light. (D) Identification of target cysteine residue on IDPm. Wild-type and mutant IDPm proteins were untreated (shaded bars) or treated with 50 (open bars) and 100 μ M (dotted bars) curcumin for 1 h at 37°C, and the remaining activity was determined. Activities are given as a percentage of the control value. Data are presented as means \pm SD of three separate experiments. (E) Inactivation of IDPm in curcumin-treated HCT116 cells. HCT116 cells were incubated with various concentrations of curcumin for 24 h and disrupted by sonication. The mitochondrial fraction was prepared and the activity of IDPm was determined. Activities are given as a percentage of the control value. Data are presented as means \pm SD of five separate experiments. (F) Inactivation of IDPm in NAC (10 mM, 24 h)-pre-treated HCT116 cells exposed to 40 μ M curcumin for 24 h. Activities are given as a percentage of the control value. Data are presented as means \pm SD of three separate experiments. * $p < 0.01$ vs cells exposed to curcumin.

cysteine residue was involved in the inactivation of IDPm by curcumin, IDPm wild-type and cysteine mutants were treated with 50 μM curcumin for 1 h at 37°C. The activity of the C379S/C269S double mutant and the C379S mutant was not affected by curcumin, but the C269S mutant was inhibited by curcumin to the same degree as wild-type IDPm (Figure 1D). Therefore, we suggest that Cys³⁷⁹ is a target for the inhibition of IDPm by curcumin. A concentration-dependent inhibition of IDPm in HCT116 cells was observed when cells were treated with various concentrations of curcumin for 24 h (Figure 1E). The treatment of the thiol antioxidant NAC protected the curcumin-induced inactivation of IDPm in HCT116 cells (Figure 1F). In animal and human studies, curcumin undergoes metabolic conjugation which generates major metabolites such as curcumin glucuronide and curcumin sulphate [32]. The effect of curcumin conjugates on the activity of enzyme containing sulphhydryl groups remains under investigation.

The knockdown of gene expression by siRNA is a powerful tool for the study of gene function *in vivo* [33]. To examine the role of IDPm in curcumin-induced apoptosis, we used specific *in vitro*-transcribed siRNAs for knockdown of human IDPm in HCT116 cells. This experimental protocol was effective in decreasing IDPm protein levels (Figure 2A). The IDPm enzyme activity was also decreased by IDPm siRNA in HCT116 cells, with and without curcumin treatment (Figure 2B). When cultured cancer cell lines, such as HeLa, HCT116 and PC3, were treated

with 40 μM curcumin, a time-dependent decrease in cell viability was observed. Cancer cells transfected with IDPm siRNA were significantly more sensitive to curcumin than control cells transfected with scrambled siRNA (Figure 2C).

To evaluate the relationship between IDPm activity and curcumin-induced apoptotic cell death, the effect of transfection of the IDPm siRNA on the cellular features of apoptosis was studied. DNA fragmentation following treatment with 40 μM curcumin for 24 h was more apparent in IDPm siRNA-transfected HCT116 cells than in control cells (Figure 3A). Figure 3B shows a typical cell cycle histogram of HCT116 cells, in which apoptotic cells can be estimated by calculating the number of sub-diploid cells. When cells were exposed to curcumin, the number of apoptotic cells was increased markedly in IDPm siRNA-transfected cells compared to control cells. These results suggest that IDPm provides some protection from curcumin-induced apoptosis. Previous studies have identified caspases as important mediators of apoptosis induced by a range of apoptotic stimuli [34]. In HCT116 cells, caspase-3 activity was significantly increased in IDPm siRNA-transfected cells compared to control cells (Figure 3C). Caspase-3 activation in this experimental system was further evaluated by measuring caspase-3 substrates and their cleavage using immunoblotting. Accumulation of PARP and lamin B cleavage fragments was apparent in IDPm siRNA-transfected cells (Figure 3D), thus confirming the activation of

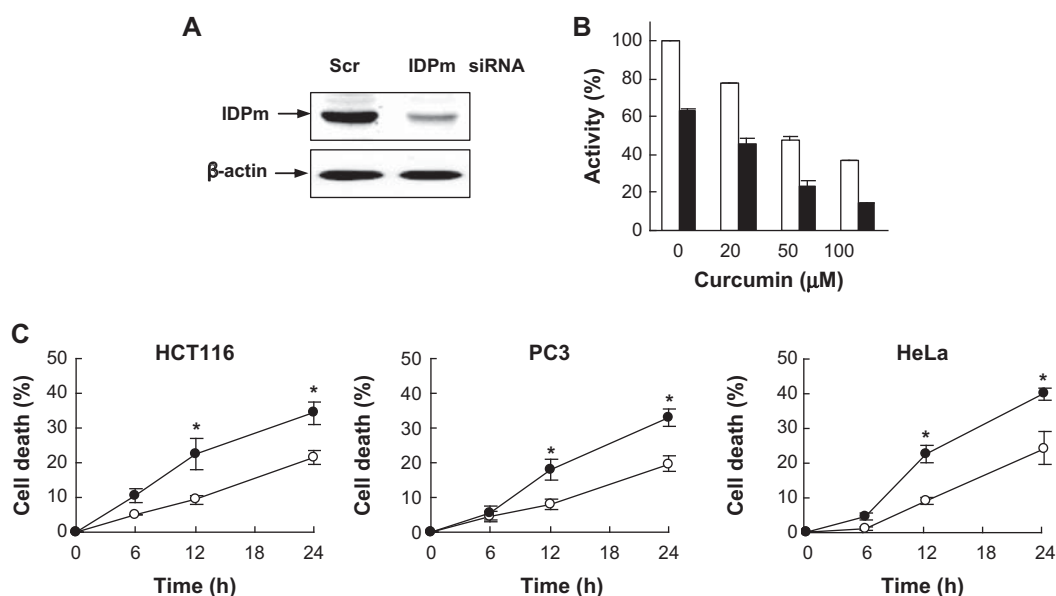


Figure 2. Knockdown of IDPm by siRNA and viability of cancer cells. HCT116 cells were transfected with scrambled siRNA (control) or IDPm siRNA. After exposure to 40 μM curcumin for 24 h, the transfected cells were disrupted by sonication and then protein levels (A) and the activity (B) of IDPm were determined. Open and shaded bars represent HCT116 cells transfected with scrambled siRNA and IDPm siRNA, respectively. Data are presented as means \pm SD of three separate experiments. (C) Viability of transfectant cancer cells exposed to curcumin. After IDPm siRNA-(closed circles) or control scrambled siRNA-transfected (open circles) HCT116, PC3, HeLa cells were exposed to 40 μM curcumin for various lengths of time at 37°C, viability of cells was determined by trypan blue exclusion assay. Data are presented as means \pm SD of three separate experiments; * $p < 0.01$ vs control cells.

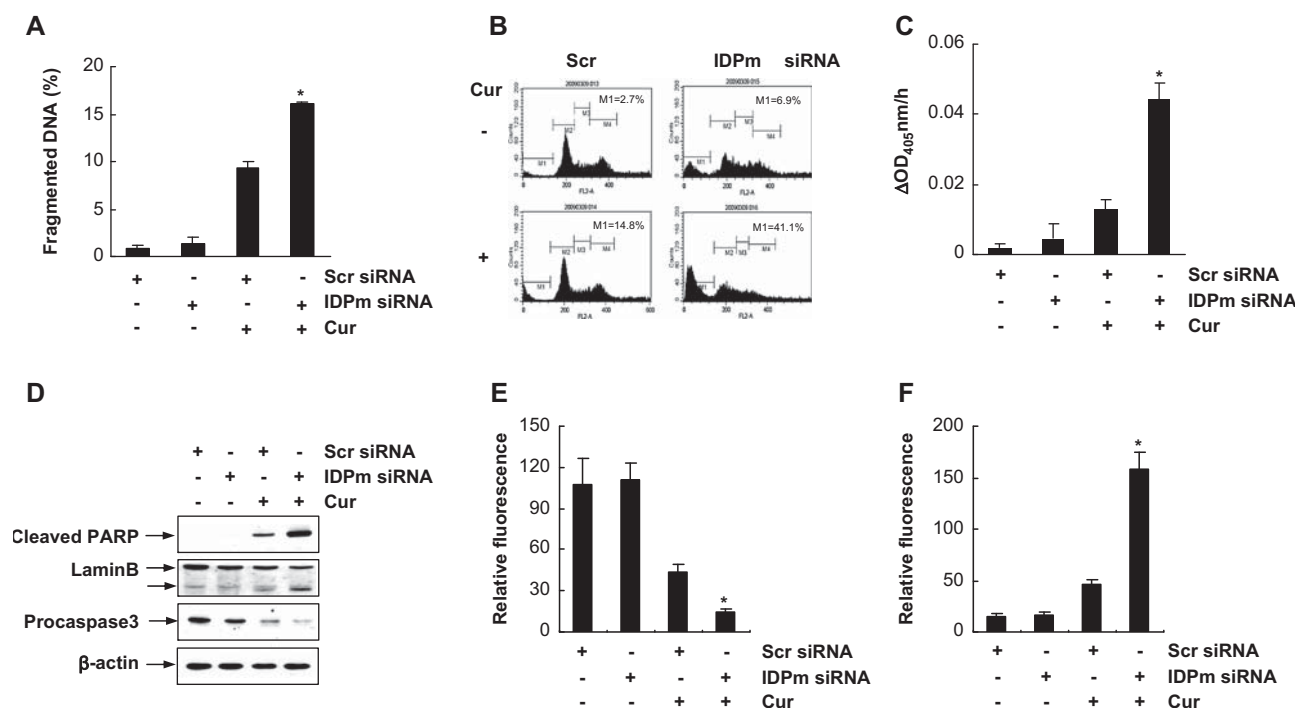


Figure 3. Curcumin-induced apoptosis in IDPm siRNA transfectant HCT116 cells. (A) DNA fragmentation was determined using diphenylamine assay. Data are presented as means \pm SD of three separate experiments; $*p < 0.01$ vs control cells exposed to curcumin. (B) Cell cycle analysis with cellular DNA content was examined by flow cytometry. The sub- G_1 region (presented as 'M1') includes cells undergoing apoptosis. The number of each panel refers to the percentage of apoptotic cells. (C) Activation of caspase-3 in HCT116 transfectant cells exposed to 40 μ M curcumin for 24 h. HCT116 cells were lysed and centrifuged. The supernatant was then added to DEVD-pNA and subjected to caspase colourimetric activity. Protease activity of caspase-3 was calculated by monitoring the absorbance at 405 nm. Data are presented as means \pm SD of three separate experiments. $*p < 0.01$ vs control cells exposed to curcumin. (D) Immunoblot analysis of various apoptosis-related proteins in HCT116 transfectant cells unexposed or exposed to 40 μ M curcumin for 24 h. Cell extracts were subjected to 10–12.5% SDS-PAGE and immunoblotted with antibodies against cleaved caspase-3, cleaved PARP, and lamin B. β -Actin was run as an internal control. (E) Effect of IDPm siRNA on MPT. MPT of HCT116 transfectant cells was measured by the incorporation of rhodamine123 dye into the mitochondria. Fluorescence images were obtained under microscopy. (F) Effect of IDPm siRNA on mitochondrial ROS generation. DHR 123 was employed to detect mitochondrial ROS. Fluorescence images were obtained under microscopy. The averages of fluorescence intensity were calculated as described [23]. Data are presented as means \pm SD of three separate experiments. $*p < 0.01$ vs control cells exposed to curcumin.

caspase-3, the main protease responsible for PARP and lamin B cleavage.

ROS are one of the major stimuli that change mitochondrial integrity, an effect that is reflected by alterations in MPT [35]. To determine whether IDPm siRNA transfection modulates the MPT upon exposure to curcumin, we assessed the change in MPT by measuring the intensity of rhodamine 123 fluorescence. In this assay, high fluorescence indicates healthy mitochondria. Significantly less rhodamine 123 dye was taken up by the mitochondria of IDPm siRNA-transfected cells compared to control cells (Figure 3E). In order to associate the changes in MPT with ROS in mitochondria, the levels of mitochondrial ROS in HCT116 cells were evaluated using the oxidant-sensitive probe DHR 123. The intensity of fluorescence was markedly increased in IDPm siRNA-transfected cells compared to that in the mitochondria of control cells when HCT116 cells were exposed to curcumin (Figure 3F).

In order to investigate whether the difference in apoptotic cell death between control and IDPm

siRNA-transfected cells upon exposure to curcumin was associated with ROS formation, the levels of intracellular peroxides in the HCT116 cells were evaluated by confocal microscopy using the specific oxidation-sensitive fluorescent probe DCFH-DA. When HCT116 cells were treated with 40 μ M curcumin for 24 h, the increase of DCF was significantly enhanced in IDPm siRNA-transfected cells as compared to control cells (Figure 4A). NADPH, required for GSH generation by glutathione reductase, is an essential factor for the cellular defence against oxidative damage. The ratio for [NADPH]/[NADP⁺ + NADPH] was significantly decreased in cells treated with curcumin and the decrease in this ratio was much more pronounced in IDPm siRNA-transfected cells (Figure 4B). When the cells were exposed to curcumin, the ratio for [GSSG]/[GSH]_i was higher in HCT116 cells transfected with IDPm siRNA compared to that of control (Figure 4C). In order to determine whether the observed increase in ROS generation and caspase-3 activation had any relevance in IDPm siRNA-transfected cells exposed to

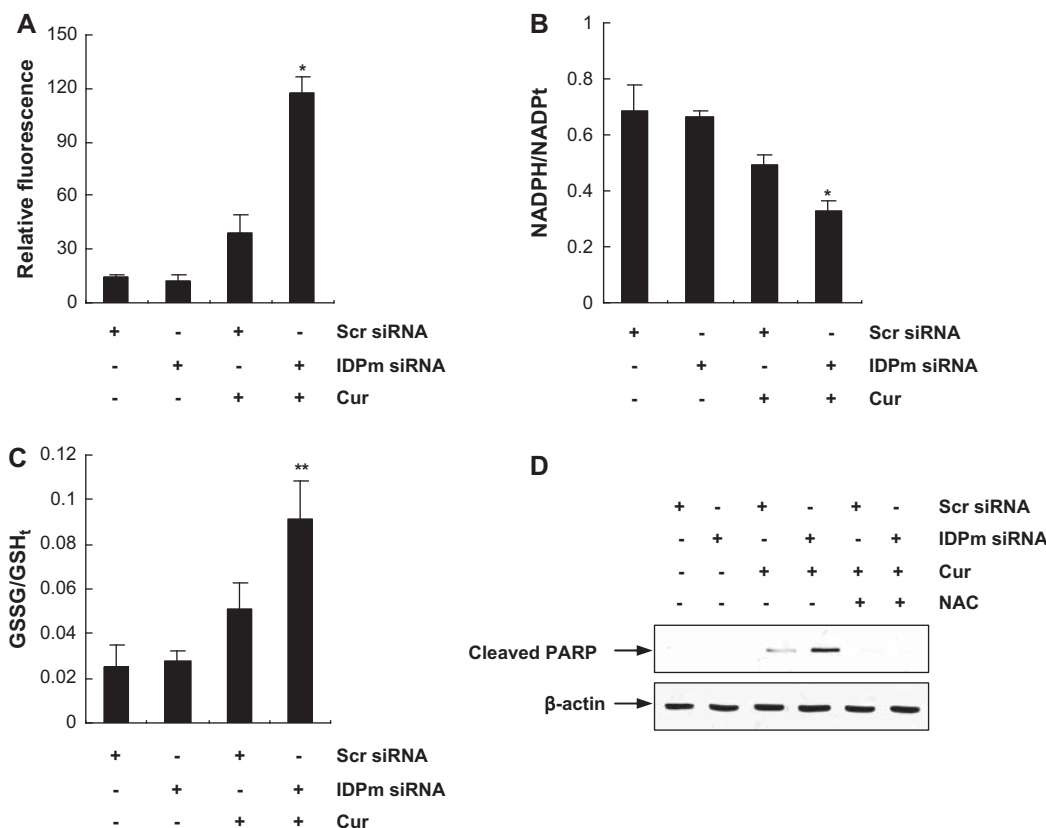


Figure 4. Cellular redox status of HCT116 transfectant cells exposed to curcumin. (A) Measurement of *in vivo* molecular oxidation. DCF fluorescence was measured in HCT116 transfected cells exposed to curcumin by confocal microscope. The averages of fluorescence intensity were calculated as described [23]. Data are presented as means \pm SD of three separate experiments. * $p < 0.01$ vs control cells exposed to curcumin. (B) NADPH vs total NADP pool in HCT116 transfectant cells exposed to 40 μ M curcumin for 24 h. Data are presented as means \pm SD of five separate experiments. * $p < 0.01$ vs control cells exposed to curcumin. (C) GSSG vs total GSH pool in HCT116 transfectant cells. Data are presented as means \pm SD of three separate experiments. ** $p < 0.05$ vs control cells exposed to curcumin. (D) Immunoblot analysis of cleaved PARP in NAC-pretreated (10 mM, 24 h) HCT116 transfectant cells exposed to 40 μ M curcumin for 24 h. β -Actin was run as an internal control.

curcumin, the effect of NAC was examined. Pre-treatment with 10 mM NAC for 24 h suppressed the modulation of apoptotic marker proteins in IDPm siRNA-transfected HCT116 cells exposed to 40 μ M curcumin (Figure 4D).

In conclusion, the present work shows that curcumin can inhibit IDPm activity by modifying the sulphhydryl group of Cys³⁷⁹. Inhibition of IDPm, which will affect the antioxidant defense system via attenuation of NADPH generation, is a potential mechanism contributing to the anti-tumour effects of curcumin. IDPm siRNA transfection was also effective in sensitizing HCT116 cells to curcumin-induced apoptotic cell death, alterations in cellular redox status and mitochondrial dysfunction. Sensitization to curcumin-induced apoptosis by IDPm siRNA transfection may have significance in cancer treatment. During consecutive chemotherapy, the development of resistance to apoptosis in the cancer cells is a major cause of treatment failure. Thus, the combination of curcumin and IDPm siRNA may be a novel modality for improving the therapeutic ratio of chemotherapy.

Declaration of interest

This work was supported by National Research Foundation of Korea Grant funded by the Korean Government (2010-0001936 and 2010-0021563).

References

- [1] Aggarwal BB, Kumar A, Bharti AC. Anticancer potential of curcumin: preclinical and clinical studies. *Anticancer Res* 2003;23:363–398.
- [2] Duvoix A, Blasius R, Delhalle S, Schnekenburger M, Morceau F, Henry E, Dicato M, Diederich M. Chemopreventive and therapeutic effects of curcumin. *Cancer Lett* 2005;223:181–190.
- [3] Ammon HP, Safayhi H, Mack T, Sabieraj J. Mechanism of antiinflammatory actions of curcumin and boswellic acids. *J Ethanopharmacol* 1993;38:113–119.
- [4] Donatus IA, Sardjoko, Vermeulen NP. Cytotoxic and cytoprotective activities of curcumin. Effects on paracetamol-induced cytotoxicity, lipid peroxidation and glutathione depletion in rat hepatocytes. *Biochem Pharmacol* 1990;39:1869–1875.
- [5] Simon A, Allais DP, Duroux JL, Basly JP, Durand-Fontanier S, Delage C. Inhibitory effect of curcuminoids on MCF-7 cell proliferation and structure-activity relationships. *Cancer Lett* 1998;129:111–116.

- [6] Huang MT, Lou YR, Ma W, Newmark HL, Reuhl KR, Conney AH. Inhibitory effects of dietary curcumin on forestomach, duodenal, and colon carcinogenesis in mice. *Cancer Res* 1999;54:5841–5847.
- [7] Anto RJ, Mukhopadhyay A, Dennings K, Aggarwal BB. Curcumin (diferuloylmethane) induces apoptosis through activation of caspase-8, BID cleavage and cytochrome c release: its suppression by ectopic expression of Bcl-2 and Bcl-xl. *Carcinogenesis* 2002;23:143–150.
- [8] Joe B, Vijaykumar M, Lokesh BR. Biological properties of curcumin-cellular and molecular mechanism of action. *Crit Rev Food Sci Nutr* 2004;44:97–111.
- [9] Fang J, Lu J, Holmgren A. Thioredoxin reductase is irreversibly modified by curcumin. *J Biol Chem* 2005;280:25284–25290.
- [10] Vaux DL, Korsmeyer SJ. Cell death in development. *Cell* 1999;96:245–254.
- [11] Fang J, Nakamura H, Iyer AK. Tumor-targeted induction of oxystress for cancer therapy. *J Drug Targeting* 2007;15:475–486.
- [12] Miller AF. Superoxide dismutases: active sites that save, but a protein that kills. *Curr Opin Chem Biol* 2004;8:162–168.
- [13] Dickinson DA, Forman HJ. Glutathione in defense and signaling: lessons from a small thiol. *Ann NY Acad Sci* 2002;973:488–504.
- [14] Cox AG, Winterbourn CC, Hampton MB. Mitochondrial peroxiredoxin involvement in antioxidant defence and redox signaling. *Biochem J* 2009;425:313–328.
- [15] Avery AM, Willetts SA, Avery SV. Genetic dissection of the phospholipid hydroperoxidase activity of yeast gpx3 reveals its functional importance. *J Biol Chem* 2004;279:46652–46658.
- [16] Outten CE, Culotta VC. Alternative start sites in the *Saccharomyces cerevisiae* GLR1 gene are responsible for mitochondrial and cytosolic isoforms of glutathione reductase. *J Biol Chem* 2004;279:7785–7791.
- [17] Lillig CH, Lonn ME, Enoksson M, Fernandes AP, Holmgren A. Short interfering RNA-mediated silencing of glutaredoxin 2 increases the sensitivity of HeLa cells toward doxorubicin and phenylarsine oxide. *Proc Natl Acad Sci USA* 2004;101:13227–13232.
- [18] Koshland DE, Walsh K, LaPorte DC. Sensitivity of metabolic fluxes to covalent control. *Curr Top Cell Regul* 1985;27:13–22.
- [19] Jo SH, Son MK, Koh HJ, Lee SM, Song IH, Kim YO, Lee YS, Jeong KS, Kim WB, Park J-W, Song BJ, Huh TL. Control of mitochondrial redox balance and cellular defense against oxidative damage by mitochondrial NADP⁺-dependent isocitrate dehydrogenase. *J Biol Chem* 2001;276:16168–16176.
- [20] Hoffmann A, Roeder RG. Purification of his-tagged proteins in non-denaturing conditions suggests a convenient method for protein interaction studies. *Nucl Acid Res* 1991;19:6337–6338.
- [21] Zerez CR, Lee SJ, Tanaka KR. Spectrophotometric determination of oxidized and reduced pyridine nucleotides in erythrocytes using a single extraction procedure. *Anal Biochem* 1987;164:367–373.
- [22] Anderson ME. Determination of glutathione and glutathione disulfide in biological samples. *Methods Enzymol* 1985;113:548–555.
- [23] Tak JK, Park J-W. The use of ebselen for radioprotection in cultured cells and mice. *Free Radic Biol Med* 2009;46:1177–1185.
- [24] Shin AH, Kil IS, Yang ES, Huh TL, Yang CH, Park J-W. Regulation of high glucose-induced apoptosis by mitochondrial NADP⁺-dependent isocitrate dehydrogenase. *Biochem Biophys Res Commun* 2004;325:32–38.
- [25] Kim HJ, Kang BS, Park J-W. Cellular defense against heat shock-induced oxidative damage by mitochondrial NADP⁺-dependent isocitrate dehydrogenase. *Free Radic Res* 2005;39:441–448.
- [26] Lee JH, Kim SY, Kil IS, Park J-W. Regulation of ionizing radiation-induced apoptosis by mitochondrial NADP⁺-dependent isocitrate dehydrogenase. *J Biol Chem* 2007;282:13385–13394.
- [27] Lee JH, Park J-W. Oxalomalate regulates ionizing radiation-induced apoptosis in mice. *Free Radic Biol Med* 2007;42:44–51.
- [28] Kil IS, Kim SY, Lee SJ, Park J-W. Small interfering RNA-mediated silencing of mitochondrial NADP⁺-dependent isocitrate dehydrogenase enhances the sensitivity of HeLa cells toward tumor necrosis factor- α and anticancer drugs. *Free Radic Biol Med* 2007;43:1197–1207.
- [29] Smyth GE, Colman RF. Cysteinyl peptides of pig heart NADP-dependent isocitrate dehydrogenase that are modified upon inactivation by N-ethylmaleimide. *J Biol Chem* 1991;266:14918–14925.
- [30] Fatania HR, al-Nassar KE, Thomas N. Chemical modification of rat liver cytosolic NADP(+)-linked isocitrate dehydrogenase by N-ethylmaleimide. Evidence for essential sulphhydryl groups. *FEBS Lett* 1993;322:245–248.
- [31] Johanson RA, Colman RF. Cysteine in the manganous-isocitrate binding site of pig heart TPN-specific isocitrate dehydrogenase. II. Identification of a critical cysteine-containing tryptic peptide derived from the thiocyanate enzyme. *Arch Biochem Biophys* 1981;207:21–31.
- [32] Vareed SK, Kakarata M, Ruffin MT, Crowell JA, Normollo DP, Djuric Z, Brenner DE. Pharmacokinetics of curcumin conjugate metabolites in healthy human subjects. *Cancer Epidemiol Biomarkers Prev* 2008;17:1411–1417.
- [33] Juliano R, Alam MR, Dixit V, Kang H. Mechanisms and strategies for effective delivery of antisense and siRNA oligonucleotides. *Nucl Acid Res* 2008;36:4158–4171.
- [34] Creagh EM, Martin SJ. Caspases: cellular demolition experts. *Biochem Soc Trans* 2001;29:696–702.
- [35] Pastorino JG, Simbula G, Yamamoto K, Glascott PA, Rothman RJ, Farber JL. The cytotoxicity of tumor necrosis factor depends on induction of the mitochondrial permeability transition. *J Biol Chem* 1996;271:29792–29798.

This paper was first published online on Early Online on 1 December 2010.